Electronic Supplementary Material (ESI) for Physical Chemistry Chemical Physics.

Supplementary Information: Shedding Light on the Different Behavior of Ionic and Nonionic Surfactants in Emulsion Polymerization: From Atomistic Simulations to Experimental Observations

Giulia Magi Meconi[1], Nicholas Ballard[1], José M. Asua[1], and Ronen Zangi*[2,3]

[1]POLYMAT & Departamento de Química Aplicada, Facultad de Ciencias Químicas, University of the Basque Country UPV/EHU, Avenida de Tolosa 72, 20018, Donostia–San Sebastián, Spain

[2]POLYMAT & Departamento de Química Orgánica I, University of the Basque Country UPV/EHU, Avenida de Tolosa 72, 20018, Donostia–San Sebastián, Spain

[3]IKERBASQUE, Basque Foundation for Science, María Díaz de Haro 3, 48013 Bilbao, Spain

October 31, 2017

*Email: r.zangi@ikerbasque.org

Table S1: Details of the simulations for the five organic phases (different composition of PS and styrene) studied. For each organic phase, we considered four concentrations (eleven for 100% S) of 10PEO6PE surfactants. The average lengths of the simulation box along each axis are indicated (the interfaces between water and the organic phase are normal to the z-axis). The values of the 2D-densities, ρ_{2D}, are initial values which do not take into consideration absorption into the organic phase at equilibrium. For the system with 100% S the box lengths in the x- and y-axes are the same.

	# 16-mer PS	# S	# 10PEO6PE	ρ_{2D} [mg/m^2]	# Waters	$\langle X \rangle$ [nm]	$\langle Y \rangle$	$\langle Z \rangle$ [nm]
100% S	0	2304	0	0	8170	5.17	5.17	25.00
	0	2304	2	0.0405	8170	5.18	5.18	25.00
	0	2304	6	0.121	8170	5.20	5.20	25.00
	0	2304	8	0.161	8170	5.20	5.20	25.00
	0	2304	12	0.240	8170	5.22	5.22	25.00
	0	2304	18	0.378	8604	5.09	5.09	27.00
	0	2304	20	0.419	8604	5.10	5.10	27.00
	0	2304	30	0.619	8604	5.13	5.13	27.00
	0	2304	40	0.814	8604	5.17	5.17	27.00
	0	2304	80	1.53	11630	5.33	5.33	30.00
	0	2304	120	2.20	11630	5.45	5.45	30.00
25% PS / 75% S	36	1728	0	0	14208	5.64	6.74	22.00
	36	1728	18	0.244	15130	5.79	6.92	22.00
	36	1728	62	0.826	14208	5.84	6.99	22.00
	36	1728	122	1.66	11628	5.79	6.92	22.00
50% PS / 50% S	72	1152	0	0	13036	6.66	5.65	21.00
	72	1152	18	0.255	13036	6.73	5.71	21.00
	72	1152	56	0.767	12678	6.84	5.81	21.00
	72	1152	114	1.56	13308	6.83	5.80	23.00

Continued on next page

Table S1 – continued from previous page

	# 16-mer PS	# S	# 10PEO6PE	ρ_{2D} [mg/m^2]	# Waters	$\langle X \rangle$ [nm]	$\langle Y \rangle$	$\langle Z \rangle$ [nm]
75% PS / 25% S	108	576	0	0	14392	6.79	5.50	22.00
	108	576	18	0.256	14392	6.87	5.56	22.00
	108	576	62	0.875	13138	6.90	5.59	22.00
	108	576	124	1.70	11892	7.00	5.67	22.00
100% PS	144	0	0	0	13238	6.35	5.94	21.00
	144	0	18	0.252	13238	6.45	6.03	20.84
	144	0	56	0.779	12148	6.47	6.04	20.86
	144	0	112	1.56	10404	6.45	6.03	21.00

Table S2: Details of the simulation setups for the SDS surfactants studied at two different 2D-densities with 100% S as the organic phase. The data collection time was 20 ns, and the equilibration time was 80 and 100 ns for the systems with 146 and 200 SDSs, respectively. The box lengths in the x- and y-axes are the same.

# SDS	ρ_{2D} [mg/m^2]	# S	# Waters	$\langle X \rangle / \langle Y \rangle$ [nm]	$\langle Z \rangle$ [nm]
146	1.24	2304	5286	5.31	22.80
200	1.65	2304	5203	5.39	22.80

Table S3: Details of the simulation setups for the calculations of the potential of mean force of pulling one 10PEO6PE surfactant adsorbed at the interface to the water phase. The different densities, reported as ρ_{2D}, correspond to different numbers of surfactants initially placed at the interface.

# 10PEO6PE	ρ_{2D} [mg/m^2]	# S	# Waters	$\langle X \rangle / \langle Y \rangle$ [nm]	$\langle Z \rangle$ [nm]
1	0.0538	384	4113	4.50	9.70
8	0.453	384	11452	4.38	22.04
12	0.686	384	8006	4.36	17.05

Models for Styrene and Poly(styrene)

The bonded and non-bonded parameters for styrene and PS were taken from the OPLS-AA force-field of ethylbenzene and ethylene molecules.[1–3] However for PS, in order to allow the connectivity between the subunits and simultaneously maintain zero charge for each of these subunits, we made the following changes. The partial charge of C_β of the first residue was changed from -0.180 to -0.120, that of C_γ of the last residue was changed from -0.115 to -0.055, and both changes were applied to the repeating residues. The chain of PS is modeled as a 16-mer unit. Because the stereochemistry of each unit is randomly generated during polymerization, we chose to model each chain with alternating C_α chiral centers (R followed by S). The resulting model is shown in Fig. S1 and the non-bonded interactions are specified in Table S4. Using this model, we obtained a value of 1.02 kg/m^3 for the density of amorphous PS which is close to its experimental value[4] of 1.04–1.06 kg/m^3. Furthermore, the calculated values of the radius of gyration, 9.8 Å, and the weight-normalized end-to-end distance squared, 0.42 Å$^2\cdot$ mol/g, are also in a very good agreement with their experimentally determined values of 10.0 Å and 0.43 Å$^2\cdot$ mol/g, respectively.

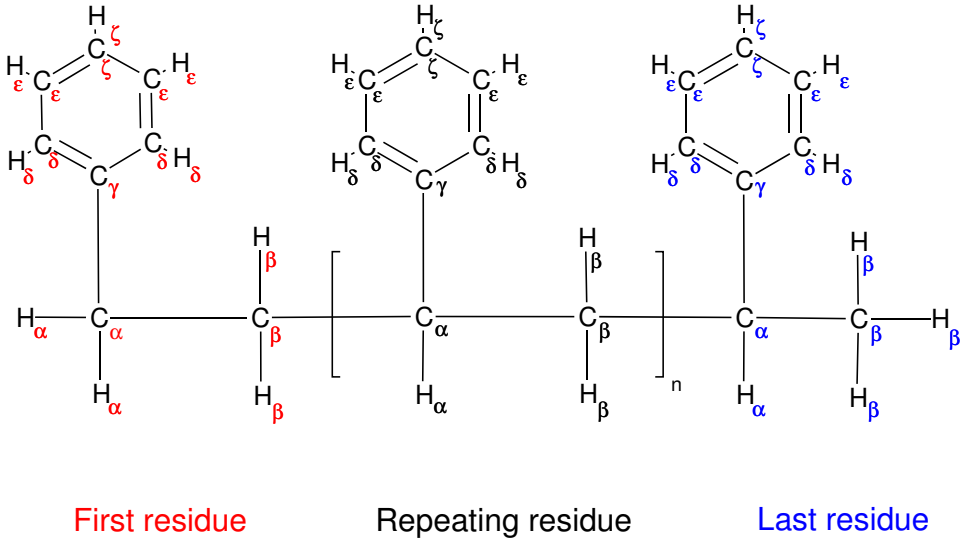

Figure S1: The model for PS based on the OPLS-AA force-field. The partial charge and LJ parameters describing each atom are detailed in Table S4. Note that the C_α of the repeating and last residues are chirals, nevertheless, the parameters for the R and S configurations are the same.

Table S4: Partial charges and LJ parameters for the PS model. The values refer to all residue types (first, repeating, and last) unless otherwise indicated.

	q [e]	σ [nm]	ϵ [kJ/mol]
C_α	-0.005	0.350	0.276
C_β	-0.120	0.350	0.276
$C_{\beta,\text{last}}$	-0.180	0.350	0.276
C_γ	-0.055	0.355	0.293
$C_{\gamma,\text{first}}$	-0.115	0.355	0.293
H_α, H_β	+0.060	0.250	0.126
C_δ, C_ϵ, C_ζ	-0.115	0.355	0.293
H_δ, H_ϵ, H_ζ	+0.115	0.242	0.126

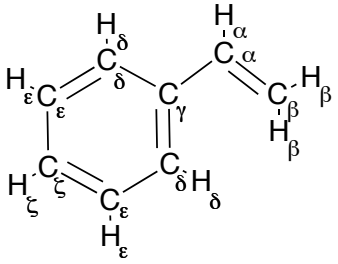

Figure S2: The model for a styrene molecule. The OPLS-AA partial charges and LJ parameters are detailed in Table S5.

Table S5: Partial charges and LJ parameters for styrene.

	q [e]	σ [nm]	ϵ [kJ/mol]
C_α	-0.115	0.355	0.318
C_β	-0.230	0.355	0.318
C_γ	-0.115	0.355	0.293
H_α	+0.23	0.242	0.126
H_β	+0.115	0.242	0.126
C_δ, C_ϵ, C_ζ	-0.115	0.355	0.293
H_δ, H_ϵ, H_ζ	+0.115	0.242	0.126

A Model for poly(ethylene oxide)-poly(ethylene)

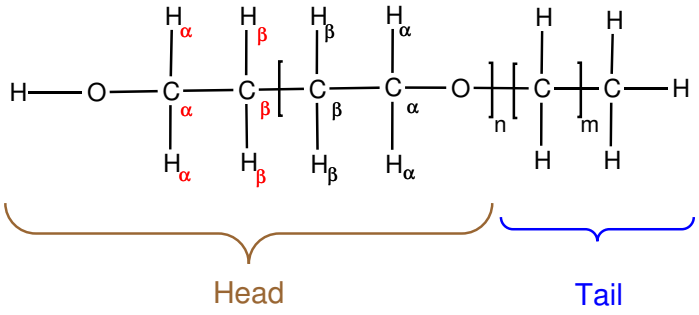

Figure S3: The model for 10PEO6PE surfactant (n=10 and m=11). The partial charges and LJ parameters, taken from the OPLS-AA force-field, are detailed in Table S6. For PEO, the values were based on a dimethyl ether.

Table S6: Partial charges and LJ parameters for the PEO-PE surfactant model. The atoms are divided according to their association to the head or tail groups.

	q [e]	σ [nm]	ϵ [kJ/mol]
Head			
$C_{\alpha,\beta}$	+0.140	0.350	0.276
$C_{\alpha,first}$	-0.015	0.350	0.276
$H_{\alpha,\beta}$	+0.030	0.250	0.126
$H_{\alpha,first}$	+0.040	0.250	0.126
O	-0.400	0.290	0.586
O_{first}	-0.683	0.312	0.711
H_{first}	+0.418	0.000	0.000
Tail			
C	-0.120	0.350	0.276
C_{last}	-0.180	0.350	0.276
H	+0.060	0.250	0.126

A Model for Sodium Dodecyl Sulfate

Partial charges, bonded and nonbonded parameters for SDS were adopted from the model of Shelley et al.[5,6]. Note that this model integrates the hydrogens of the methyl and methylene groups into the carbons to which they are connected. To obtain an all-atom representation, we represented the atom-types and partial charges of methyl and methylene groups by the OPLS-AA force-field for hydrocarbons. The sum of the charges for each of these groups is zero, therefore, in order to determine the partial charges of the first methylene group (which has a total charge of $+0.137$ e), we performed quantum calculations (using the Gaussian09 software[7] at the MP2/6-31++G**) and followed the RESP (Restrained Electrostatic Potential) charge fitting procedure[8]. Bonded interactions that were missing for the all-atom description were taken from the corresponding interactions of the OPLS-AA force-field. The resulting model is displayed in Fig. S4 and the non-bonded parameters in Table S7 The LJ parameters of the sodium counterion, σ=0.333 nm and ϵ=0.0116 kJ/mol, were taken from the OPLS-AA force-field. Note that the charges obtained by RESP reproduce the, quantum mechanically determined, electrostatic potential at large number of grid points around the optimized geometry of the molecule. Thus, their values can differ substantially from the atomic charges determined quantum mechanically (e.g, as defined by Mulliken) for the same optimized molecular structrure (see Fig. S5).

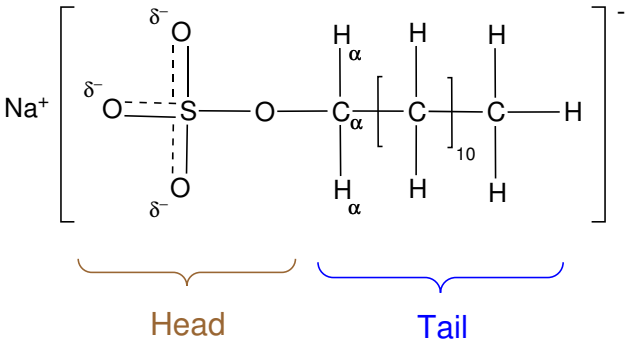

Figure S4: The model for SDS surfactant. The partial charge and LJ parameters describing each atom are detailed in Table S7.

Table S7: Partial charges and LJ parameters for the SDS model. The atoms are divided according to their association to the head or tail groups.

	q [e]	σ [nm]	ϵ [kJ/mol]
Head			
S	+1.284	0.355	1.046
O	-0.654	0.315	0.837
O_{ester}	-0.459	0.300	0.711
Tail			
C_α	+0.077	0.350	0.276
H_α	+0.030	0.242	0.063
C	-0.120	0.350	0.276
C_{last}	-0.180	0.350	0.276
H	+0.060	0.250	0.126

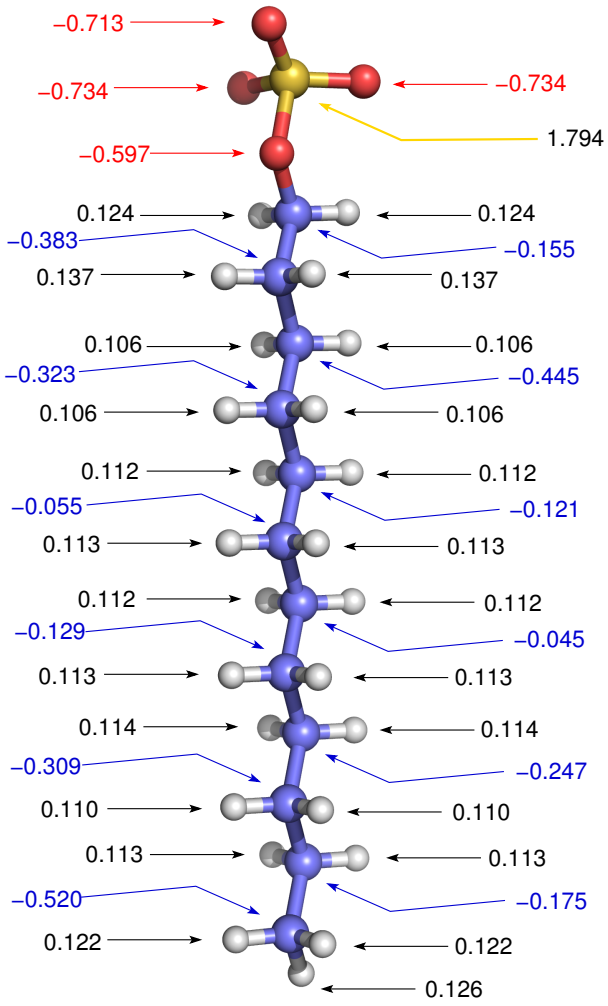

Figure S5: Atomic (Mulliken) charges (in elementary charge units, *e*) for the dodecyl sulfate anion optimized quantum mechanically at the MP2/6-31++G** level. These charges were *not* used in the classical simulations.

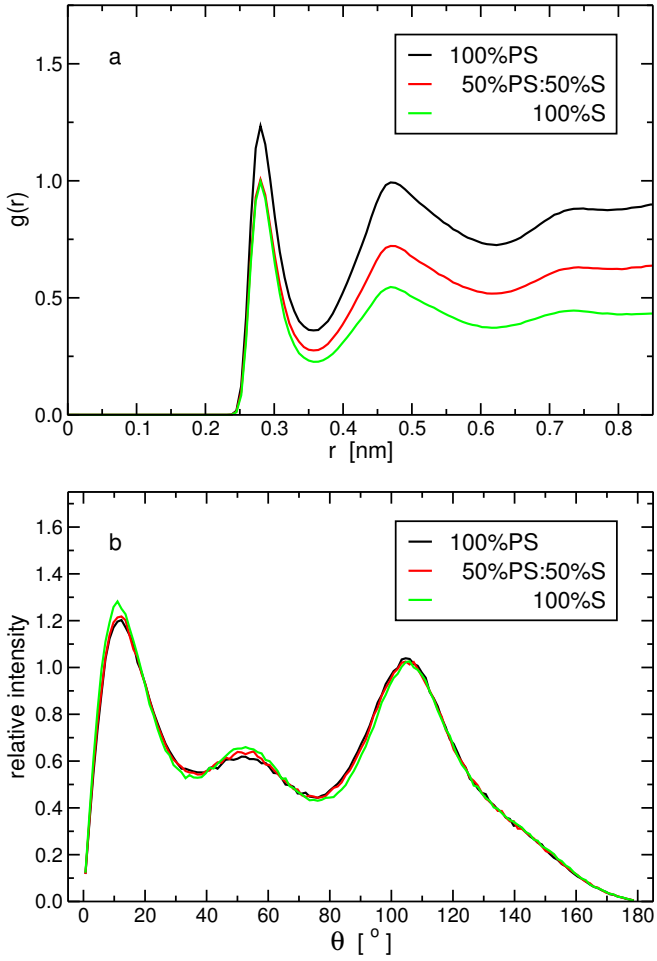

Figure S6: (a) The radial distribution function between the oxygen atoms of the nonionic surfactant and the oxygen atoms of the water molecules. (b) The distribution of the angle formed by the hydrogen–oxygen(water)–oxygen(surfactant) atomic sites for donor–acceptor distances smaller than 0.35 nm. For both plots, the corresponding distributions were calculated for three different chemical compositions of the organic phase.

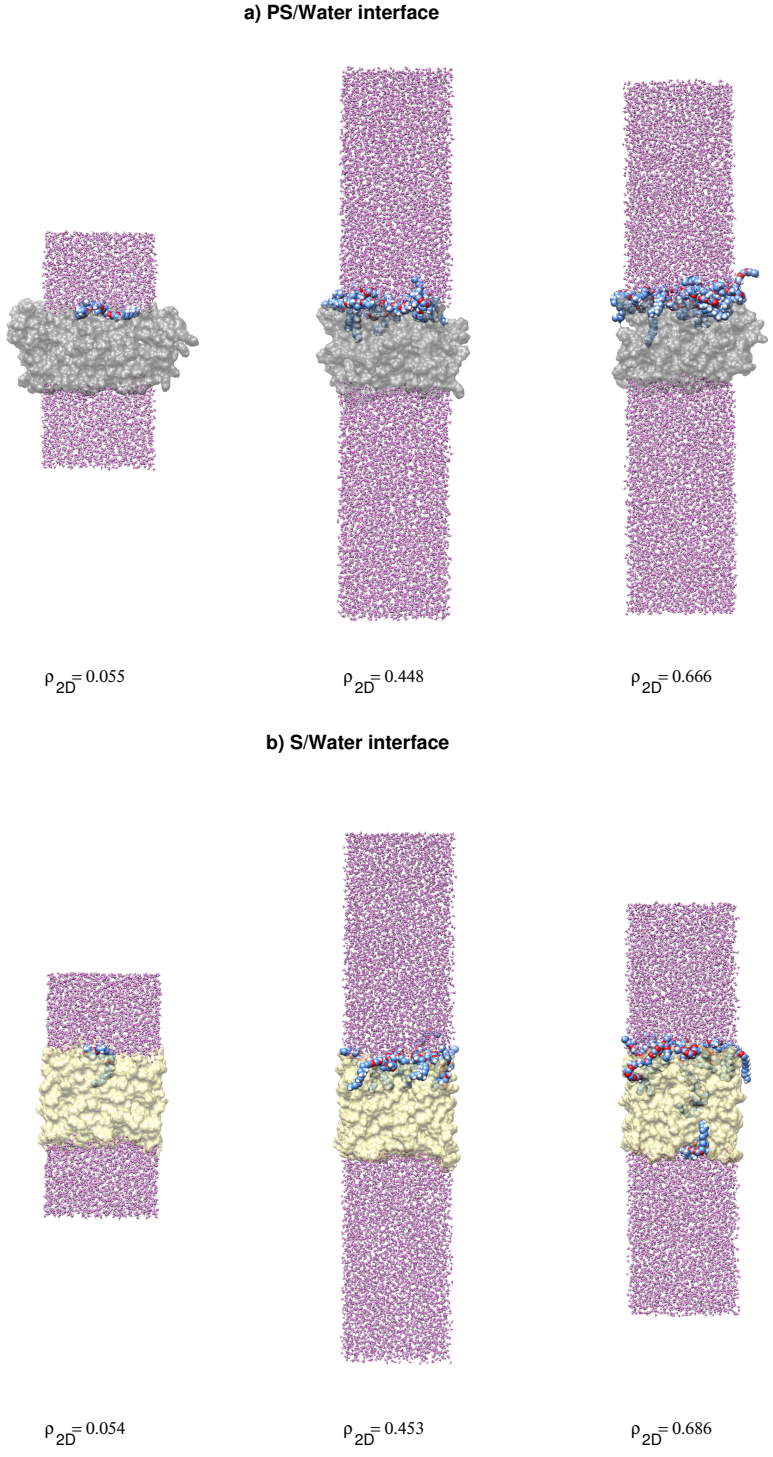

Figure S7: Same as Fig. 10, however here, the entire length of the simulation box along the z-axis (normal to the interface) is shown for all snapshots.

Relation between the Surfactant Densities at the Interface and inside the Organic Phase

The chemical potential of the surfactant in the organic phase is given by,

$$\mu_{\mathsf{op}} = \mu_{\mathsf{op}}^{\ominus} + \mathsf{RT} \ln \mathsf{a}_{\mathsf{op}} = \mu_{\mathsf{op}}^{\ominus} + \mathsf{RT} \ln \left[\gamma_{\mathsf{op}} \frac{\rho_{\mathsf{op}}}{\rho_{\mathsf{op}}^{\ominus}} \right] \quad , \tag{S1}$$

where $\mu_{\mathsf{op}}^{\ominus}$ is the chemical potential in the organic phase under standard conditions of temperature, pressure, and density. The term a_{op} is the activity of the surfactants relative to the standard state, which can be written in terms of the activity coefficient, γ_{op}, and the surfactant density relative to that chosen for the standard state. A corresponding term holds at the interface,

$$\mu_{\mathsf{int}} = \mu_{\mathsf{int}}^{\ominus} + \mathsf{RT} \ln \left[\gamma_{\mathsf{int}} \frac{\rho_{\mathsf{int}}}{\rho_{\mathsf{int}}^{\ominus}} \right] \quad . \tag{S2}$$

At equilibrium, $\mu_{\mathsf{op}} = \mu_{\mathsf{int}}$, from which we get,

$$\rho_{\mathsf{op}} = \frac{\gamma_{\mathsf{int}}}{\gamma_{\mathsf{op}}} \cdot \frac{\rho_{\mathsf{op}}^{\ominus}}{\rho_{\mathsf{int}}^{\ominus}} \exp \left[- \left(\mu_{\mathsf{op}}^{\ominus} - \mu_{\mathsf{int}}^{\ominus} \right) / \mathsf{RT} \right] \rho_{\mathsf{int}} \quad . \tag{S3}$$

The terms associated with the standard states and the activity coefficients are constants with respect to the concentration of the surfactant, and therefore, a plot of ρ_{op} as a function of ρ_{int} should yield a straight line as obtained in Fig. 12a. Note that the lines do not pass through the origin, because below the critical density the surfactant does not absorb into the organic phase and the there is no equality between the chemical potentials (i.e., Eq. S3 does not hold). In fact in this case, the chemical potential of the surfactant in the organic phase is larger than that in that at the interface.

Taking the derivative of Eq. S3 with respect to ρ_{int} on both sides of Eq. S3 yields,

$$\frac{\mathsf{d}\rho_{\mathsf{op}}}{\mathsf{d}\rho_{\mathsf{int}}} = \frac{\gamma_{\mathsf{int}}}{\gamma_{\mathsf{op}}} \cdot \frac{\rho_{\mathsf{op}}^{\ominus}}{\rho_{\mathsf{int}}^{\ominus}} \exp \left[- \left(\mu_{\mathsf{op}}^{\ominus} - \mu_{\mathsf{int}}^{\ominus} \right) / \mathsf{RT} \right] \quad , \tag{S4}$$

which can also be written as,

$$\ln \left[\frac{\mathsf{d}\rho_{\mathsf{op}}}{\mathsf{d}\rho_{\mathsf{int}}} \right] = \mu_{\mathsf{int}}^{\ominus} / \mathsf{RT} + \ln \left[\frac{\gamma_{\mathsf{int}}}{\gamma_{\mathsf{op}}} \cdot \frac{\rho_{\mathsf{op}}^{\ominus}}{\rho_{\mathsf{int}}^{\ominus}} \right] - \mu_{\mathsf{op}}^{\ominus} / \mathsf{RT} \quad . \tag{S5}$$

Note that, in principle, for different organic phases $\mu_{\mathsf{int}}^{\ominus}$ is different. Nevertheless in our systems for which the surfactant exhibits non-zero density inside the organic phase, it is almost exclusively styrene that is found at the interface with water (see Fig. 11 for 100% S, 75% S, and 50% S). Because of this observation we consider that $\mu_{\mathsf{int}}^{\ominus}$ and γ_{int} are independent of these three organic phases. In addition, we also make

the assumption that the value of γ_{op}, which represents the degree of deviation from an ideal behavior, is the same for these systems.

Under these two assumptions, Eq. S5 indicates that the natural logarithm of the slopes of the lines in Fig. 12a, for different chemical compositions of the organic phase, are only a function of $\mu^{\ominus}_{op}$ where all other terms enter as constant parameters. For an organic phase composed of styrene and PS, one may naively try to relate $\mu^{\ominus}_{op}$ to the chemical potential of styrene in the standard state, $\mu^{\ominus}_{str}$, and that of PS, $\mu^{\ominus}_{ps}$, weighted linearly by the corresponding fractions in the organic phase, χ_{str} and 1 - χ_{str}, respectively.

$$\mu^{\ominus}_{op} \simeq \chi_{str}\mu^{\ominus}_{str} + (1-\chi_{str})\mu^{\ominus}_{ps} \tag{S6}$$

In such a case, Eq. S5 becomes,

$$\ln\left[\frac{d\rho_{op}}{d\rho_{int}}\right] = \left(\mu^{\ominus}_{int} - \mu^{\ominus}_{ps}\right)/RT + \ln\left[\frac{\gamma_{int}}{\gamma_{op}}\cdot\frac{\rho^{\ominus}_{op}}{\rho^{\ominus}_{int}}\right] - \left(\mu^{\ominus}_{str} - \mu^{\ominus}_{ps}\right)/RT\cdot\chi_{str} \quad . \tag{S7}$$

Thus, plotting $\ln\left[\frac{d\rho_{op}}{d\rho_{int}}\right]$ as a function of χ_{str} should yield a straight line with a slope equals -$\left(\mu^{\ominus}_{str} - \mu^{\ominus}_{ps}\right)/RT$. This is plotted in Fig. S8 for the three organic phases containing non-zero surfactant density.

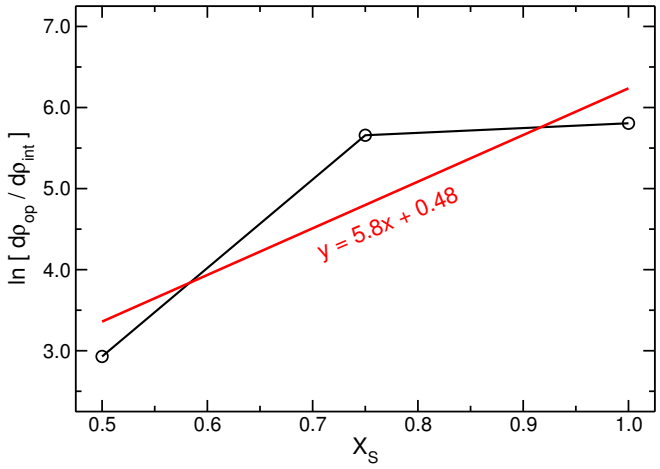

Figure S8: The natural logarithm of the slopes of the lines shown in Fig. 12a (for 100% S, 75% S, and 50% S) as a function of the mass fraction of styrene in the organic phase (see Eq. S7). Only points surrounded by orange circles in Fig. 12a are used for the calculations of the slopes. The red line is a linear regression obtained with a correlation coefficient of 0.888.

The slope of 5.8 of the linear regression means that $\mu^{\ominus}_{\mathsf{str}}$ is smaller by 5.8 RT than $\mu^{\ominus}_{\mathsf{ps}}$, which is in agreement with the observation that the surfactant absorbs significantly more in the styrene phase relative to the PS phase. Nevertheless, the relatively small correlation coefficient for the linear fitting suggests that $\mu^{\ominus}_{\mathsf{op}}$ deviates from the simplistic expression we assumed, and/or the value of γ_{op} varies for the three organic phases. In particular, for 75% S the organic phase resembles 100% S more than expected based on linear interpolation of the mass fractions of the two components, whereas for 50% S, it resembles less.

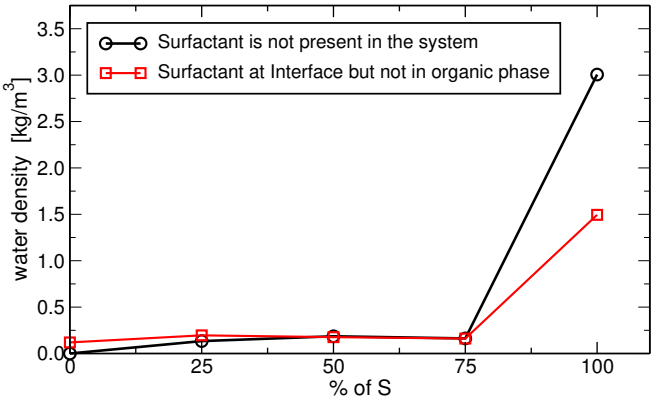

Figure S9: The density of the water molecules inside the organic phase as a function of the percentage of styrene composing the organic phase. The data are plotted for cases in which no surfactant (10PEO6PE) is either present at all in the system or absorbed inside the organic phase (but adsorb at the interface). For the latter, we chose the system with the highest density of surfactant at the interface that does not support absorbance into the organic phase.

References

[1] Jorgensen, W. L.; Severance, D. L. Aromatic-Aromatic Interactions: Free Energy Profiles for the Benzene Dimer in Water, Chloroform and Liquid Benzene, *J. Am. Chem. Soc.* **1990**, *112*, 4768–4774.

[2] Jorgensen, W. L.; Maxwell, D. S.; .; Tirado-Rives, J. Development and Testing of the OPLS All-Atom Force Field on Conformational Energetics and Properties of Organic Liquids, *J. Am. Chem. Soc.* **1996**, *118*, 11225–11236.

[3] Price, M. L. P.; Ostrovsky, D.; Jorgensen, W. L. Gas-Phase and Liquid-State Properties of Esters, Nitriles, and Nitro Compounds with the OPLS-AA Force Field, *J. Comp. Chem.* **2001**, *22*, 1340–1352.

[4] Brandrup, J.; Immergut, E. H.; Grulke, E. A. *Polymer Handbook;* Wiley: New York, fourth ed., 2003.

[5] Shelley, J.; Watanabe, K.; Klein, M. L. Simulation of a sodium dodecylsulfate micelle in aqueous solution, *Int. J. Quant. Chem.* **1990**, *38*, 103–117.

[6] Schweighofer, K. J.; Essmann, U.; Berkowitz, M. Simulation of Sodium Dodecyl Sulfate at the Water-Vapor and Water-Carbon Tetrachloride Interfaces at Low Surface Coverage, *J. Phys. Chem. B* **1997**, *101*, 3793–3799.

[7] Gaussian 09 Revision A.02. Frisch, M. J.; Trucks, G. W.; Schlegel, H. B.; Scuseria, G. E.; Robb, M. A.; Cheeseman, J. R.; Scalmani, G.; Barone, V.; Mennucci, B.; Petersson, G. A.; Nakatsuji, H.; Caricato, M.; Li, X.; Hratchian, H. P.; Izmaylov, A. F.; Bloino, J.; Zheng, G.; Sonnenberg, J. L.; Hada, M.; Ehara, M.; Toyota, K.; Fukuda, R.; Hasegawa, J.; Ishida, M.; Nakajima, T.; Honda, Y.; Kitao, O.; Nakai, H.; Vreven, T.; Montgomery, Jr., J. A.; Peralta, J. E.; Ogliaro, F.; Bearpark, M.; Heyd, J. J.; Brothers, E.; Kudin, K. N.; Staroverov, V. N.; Kobayashi, R.; Normand, J.; Raghavachari, K.; Rendell, A.; Burant, J. C.; Iyengar, S. S.; Tomasi, J.; Cossi, M.; Rega, N.; Millam, J. M.; Klene, M.; Knox, J. E.; Cross, J. B.; Bakken, V.; Adamo, C.; Jaramillo, J.; Gomperts, R.; Stratmann, R. E.; Yazyev, O.; Austin, A. J.; Cammi, R.; Pomelli, C.; Ochterski, J. W.; Martin, R. L.; Morokuma, K.; Zakrzewski, V. G.; Voth, G. A.; Salvador, P.; Dannenberg, J. J.; Dapprich, S.; Daniels, A. D.; Farkas, Ö.; Foresman, J. B.; Ortiz, J. V.; Cioslowski, J.; Fox, D. J.; Gaussian, Inc., Wallingford, CT, **2009**.

[8] Bayly, C. I.; Cieplak, P.; Cornell, W.; Kollman, P. A. A well-behaved electrostatic potential based method using charge restraints for deriving atomic charges: the RESP model, *J. Phys. Chem.* **1993**, *97*, 10269–10280.